Department of the Navy
Bureau of Ships
Contract Nonr-220(12)

Water Tunnel Tests of

# THE NACA $66_1$-012 HYDROFOIL IN NONCAVITATING AND CAVITATING FLOWS

by

Robert W. Kermeen

This research was carried out under the Bureau of Ships
Fundamental Hydromechanics Research Program
Project NS 715-102, David Taylor Model Basin



Hydrodynamics Laboratory
California Institute of Technology
Pasadena, California

Report No. 47-7
February, 1956

Approved:
M.S. Plesset

## ABSTRACT

The results of force tests on the NACA $66_1$-012 hydrofoil in noncavitating and cavitating two-dimensional flow are presented. The results of wind tunnel tests on this profile are included for comparison with the results of the noncavitating water tunnel experiments. The noncavitating experiments were made at Reynolds numbers from 0.89 to $1.65 \times 10^6$ and the cavitation experiments at Reynolds numbers of 0.89 and $1.18 \times 10^6$.


## INTRODUCTION

Two-dimensional hydrodynamic data are now available for a number of hydrofoil shapes. The force coefficients in noncavitating and cavitating flow have been obtained on simple geometrical shapes such as wedges, flat plates and circular arc hydrofoils, as well as conventional cambered airfoil shapes. Symmetrical hydrofoil shapes, such as those described in this report, are important both for lifting surfaces and for nonlifting support struts and fairings. The requirements for support struts, such as low drag, low critical cavitation number, and high strength are much the same as for lifting hydrofoils.

The NACA $66_1$-012 hydrofoil was selected as a representative example of a class of airfoil shapes which would be suitable for symmetrical hydrofoil design applications where strength is important. The NACA $66_1$-012 hydrofoil has a thickness to chord ratio of 0.12 with a critical cavitation index of approximately 0.35 at an angle of attack of zero degree. For applications where cavitation resistance is a more important consideration, a thinner hydrofoil section would be selected.

In addition, this hydrofoil shape was selected to be tested in the High Speed Water Tunnel at the Hydrodynamics Laboratory and in the

water tunnel at the Iowa Institute of Hydraulic Research in order that the results obtained in the two facilities could be compared.

## APPARATUS AND TESTS

### Hydrofoil

The hydrofoil model has a 3.30-in. chord and a 2.90-in. span. The model was made of stainless steel. The NACA $66_1$-012 hydrofoil is a symmetrical profile with a maximum thickness of 12 percent of the chord. Ordinates of the hydrofoil are given in Table I and a photograph of the model in Fig. 1.

### Water Tunnel and Test Procedure

The hydrofoil model was tested in the two-dimensional working section of the High Speed Water Tunnel. The model was mounted on a 5.0-in. diameter circular disk attached to the force balance spindle and set flush in the working section wall. There was a narrow gap of approximately 0.002 in. between the free end of the model and the working section wall. Details of the test setup, force balance, test procedure, and data reduction methods are given in Refs. 1 and 2.

### Tests

The section lift, drag, and quarter-chord pitching moment were measured for noncavitating flow at water velocities of 30, 40, 50 and 60 fps, which gave Reynolds numbers from $0.89 \times 10^6$ to $1.65 \times 10^6$. Lift, drag, and quarter-chord pitching moment were measured for cavitating flow at a velocity of 40 fps for hydrofoil attack angles from zero to 7 degrees and at 30 fps for angles of attack greater than 7 degrees. Because the hydrofoil is symmetrical, the cavitating force runs were made only at positive attack angles. In each cavitation force run the angle of attack of the model and the velocity were held constant and the cavitation number varied from noncavitating flow to full cavity flow. Photographs were taken of the cavitating hydrofoil at each test point.

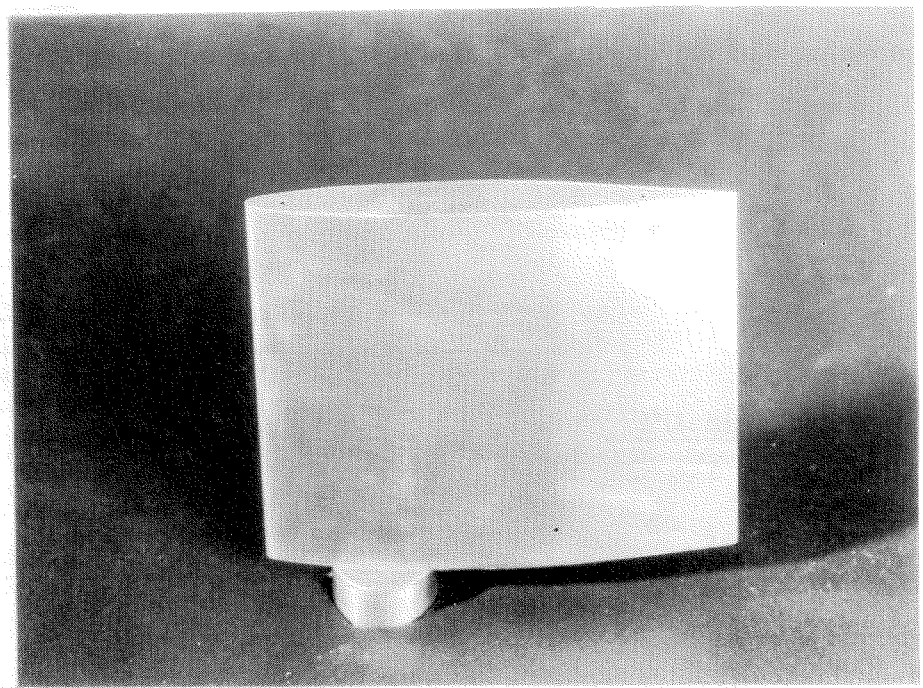

Fig. 1 - The NACA $66_1$-012 hydrofoil.

TABLE I

ORDINATES OF THE NACA $66_1$-012 HYDROFOIL

| Station % Chord | Ordinate (Upper and Lower Surface) % Chord | Station % Chord | Ordinate (Upper and Lower Surface) % Chord |
|---|---|---|---|
| 0 | 0 | 40 | 5.947 |
| 0.5 | 0.906 | 45 | 6.000 |
| 0.75 | 1.087 | 50 | 5.965 |
| 1.25 | 1.358 | 55 | 5.836 |
| 2.5 | 1.808 | 60 | 5.588 |
| 5.0 | 2.496 | 65 | 5.139 |
| 7.5 | 3.037 | 70 | 4.515 |
| 10 | 3.496 | 75 | 3.767 |
| 15 | 4.234 | 80 | 2.944 |
| 20 | 4.801 | 85 | 2.083 |
| 25 | 5.238 | 90 | 1.234 |
| 30 | 5.568 | 95 | 0.474 |
| 35 | 5.803 | 100 | 0 |

Leading Edge Radius: 0.952% Chord

## Data Reduction

The test data were reduced to dimensionless coefficients as follows:

$$\text{Lift coefficient, } C_L = \frac{\text{Lift}}{\rho/2\, V^2 A}$$

$$\text{Drag coefficient, } C_D = \frac{\text{Drag}}{\rho/2\, V^2 A}$$

$$\text{Quarter-chord pitching moment, } C_M = \frac{\text{Pitching Moment}}{\rho/2\, V^2 A c}$$

$$\text{Cavitation number, } K = \frac{P_o - P_v}{\rho/2\, V^2}$$

$$\text{Reynolds number, } Re = \frac{V c}{\nu}$$

where:

$V$ = velocity of undisturbed flow, ft/sec

$\rho$ = density of water at the temperature of the run, slugs/ft$^3$

$A$ = plan area of the hydrofoil (chord X span), ft$^2$

$c$ = chord of hydrofoil, ft

$P_o$ = pressure of undisturbed flow, lb/ft$^2$

$P_v$ = vapor pressure of fresh water at the temperature of the run, lb/ft$^2$

$\nu$ = kinematic viscosity of fresh water at the temperature of the run, ft$^2$/sec.

A number of corrections were applied to the measured data. The tare forces on the spindle disk were measured by mounting the hydrofoil from the opposite wall with a small gap between the end of the hydrofoil and the spindle disk. The force runs were repeated with this setup and the forces measured on the mounting disk alone. The lift and pitching moment disk tare corrections were negligible, hence only the

drag correction was applied to the data. The data for fully wetted flow were corrected for tunnel interference effects. The methods of data correction are described in detail in Ref. 1.

## RESULTS

Curves of lift and quarter-chord pitching moment coefficients as functions of angle of attack for noncavitating flow are shown in Fig. 2. Figure 3 is a polar diagram giving lift and drag coefficients for noncavitating flow. The results of wind tunnel tests of this profile made with the Langley two-dimensional, low-turbulence wind tunnel are shown in Figs. 2 and 3 for comparison.[3] The wind tunnel data shown are for a Reynolds number of $3.0 \times 10^6$. Figure 4 shows lift coefficient as a function of angle of attack for several cavitation numbers from fully wetted to full cavity flow. The cavitation diagram, Fig. 5, shows the extent of the cavitation on the hydrofoil as a function of angle of attack and cavitation number. Figure 7 shows lift coefficient data as a function of cavitation number at constant angles of attack. Drag coefficient is shown as a function of cavitation number at constant angles of attack in Fig. 8. Figure 9 is a cavitation polar diagram showing lift and drag coefficients for a range of cavitation numbers. Figure 10 shows the pitching moment coefficient about the quarter-chord point as a function of angle of attack and cavitation number. Lift/drag ratio is shown in Fig. 11 as a function of cavitation number and angle of attack.

## DISCUSSION OF RESULTS

### Noncavitating Flow

Lift coefficient as a function of angle of attack for noncavitating flow is shown in Fig. 2. The results of wind tunnel tests of the same profile[3] are shown for comparison. The present tests were made at Reynolds numbers from 0.89 to $1.65 \times 10^6$. The wind tunnel data are for a Reynolds number of $3.0 \times 10^6$. There are considerable

differences in Fig. 2 between the water tunnel and the wind tunnel results both in the slope of the lift coefficient curve and in the maximum lift coefficient. The lift coefficient, however, can easily change by this amount over a range of Reynolds numbers from one to three million. Data were not available for the NACA $66_1$-012 profile for Reynolds numbers less than $3.0 \times 10^6$; however, tests of a similar symmetrical NACA $64_1$-012 airfoil[4] made at Reynolds numbers from 0.7 to $9.0 \times 10^6$ show changes in lift coefficient with Reynolds number of the same magnitude as the differences between the water tunnel and wind tunnel results of Fig. 2. The NACA $64_1$-012 airfoil has a thickness of 12 percent of the chord and a profile very similar to that of the NACA $66_1$-012 profile except that the maximum thickness occurs at approximately the 40 percent chord point on the former and at the 45 percent chord point on the latter. The minimum pressure coefficient occurs at the 40 percent chord point on the NACA $64_1$-012 and at the 60 percent chord point on the NACA $66_1$-012 profile. The slope of the lift coefficient curve for the NACA $64_1$-012 profile increased from 0.099 per degree at a Reynolds number of $1.0 \times 10^6$ to 0.110 per degree at a Reynolds number of $3.0 \times 10^6$. In Fig. 2 the slope of the lift coefficient for the water tunnel data is 0.084 per degree at a Reynolds number of $1.18 \times 10^6$ and 0.105 per degree for the wind tunnel data at a Reynolds number of $3.0 \times 10^6$. The maximum lift coefficient for the NACA $64_1$-012 airfoil increased from 0.887 at a Reynolds number of $1.0 \times 10^6$ to 1.430 at a Reynolds number of $3.0 \times 10^6$ or a change of 0.543. The maximum lift coefficient for the NACA $66_1$-012 profile was 0.747 at a Reynolds number of $1.18 \times 10^6$ for the water tunnel tests and 1.222 at a Reynolds number of $3.0 \times 10^6$ for the wind tunnel tests, or an increase of 0.475.

The quarter-chord pitching moment coefficients are also shown in Fig. 2. The pitching moment coefficient does not change appreciably with Reynolds number. The curve of pitching moment coefficient from the wind tunnel tests[3] is quite different from that obtained in the water tunnel experiments. Since the hydrofoil is symmetrical, it seems reasonable that the force and moment coefficient curves should be symmetrical about zero degree attack angle. The pitching moment

coefficients about the quarter-chord point obtained in the water tunnel tests are symmetrical about zero degree and very nearly zero for angles of attack up to stall.

Figure 3 is a polar diagram showing lift and drag coefficients for noncavitating flow. At large attack angles the drag coefficient from the water tunnel tests increases rapidly due to the stall occurring at smaller attack angles than for the higher Reynolds number wind tunnel tests. In the low drag range, for lift coefficients less than $\pm 0.3$ corresponding to angle of attack of less than $\pm 3$ degrees, the water tunnel results, though somewhat higher due to smaller Reynolds numbers, are in good agreement with the wind tunnel results.

The water tunnel results show a slight increase in drag coefficient with increasing Reynolds number, indicating that a laminar boundary layer may have existed over a considerable portion of the hydrofoil. The NACA $66_1$-012 profile has its minimum pressure coefficient occurring at the 60 percent chord point at zero degree attack angle. At small attack angles the large region of decreasing pressure over the forward part of the profile would tend to delay laminar turbulent boundary layer transition and would cause an increase in drag coefficient with Reynolds number due to the laminar turbulent boundary layer transition point moving forward on the profile as the velocity is increased.

## Cavitating Flow

Lift, drag, and quarter-chord pitching moment were measured for the NACA $66_1$-012 hydrofoil for a range of cavitation numbers from fully wetted to full cavity flow at angles of attack of 0 to 10 degrees. The tests were made at a tunnel velocity of 40 fps for angles of attack up to 7 degrees and at 30 fps for attack angles greater than 7 degrees. Because the hydrofoil is symmetrical, the data are presented only for positive attack angles. No tunnel interference corrections have been applied to the data from the cavitation force runs. The cavitation number in all figures is based on the vapor pressure of water.

Figure 4 shows curves of lift coefficient as a function of angle of attack at constant cavitation numbers. The curve marked $K > 3.0$ is

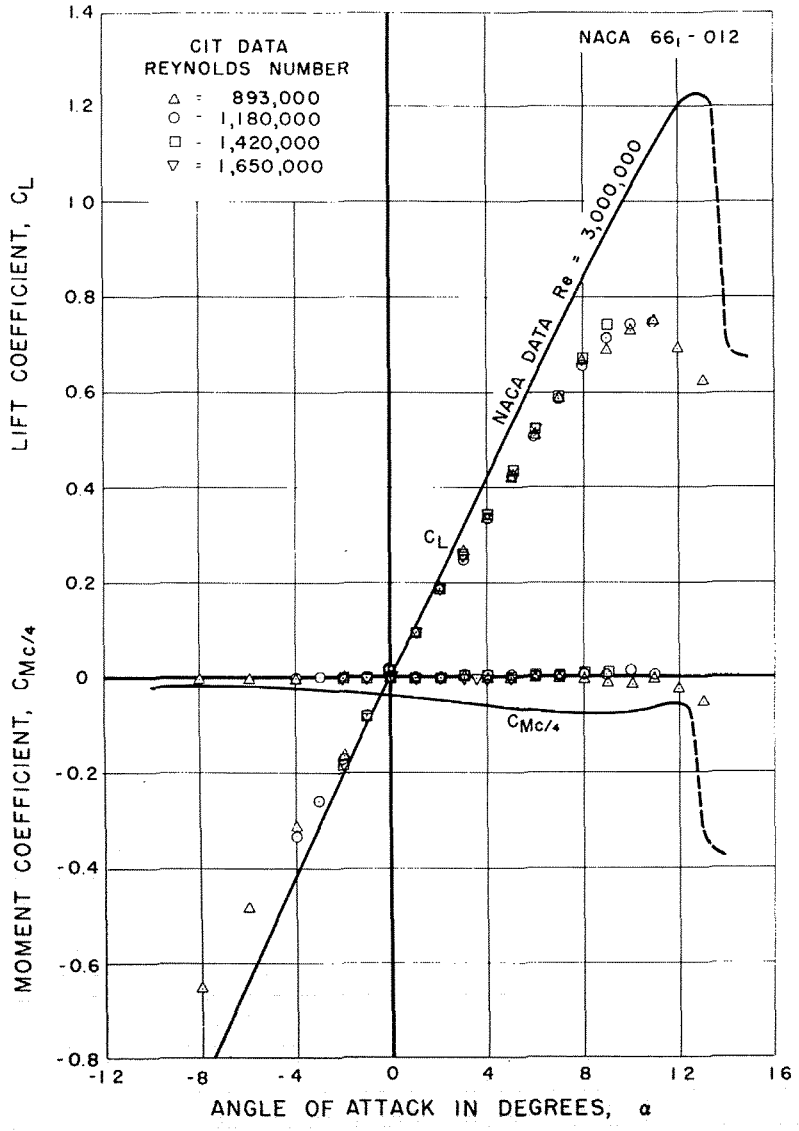


Fig. 2 - Lift coefficient and quarter-chord moment coefficient as functions of angle of attack for the NACA $66_1$-012 hydrofoil in noncavitating flow.

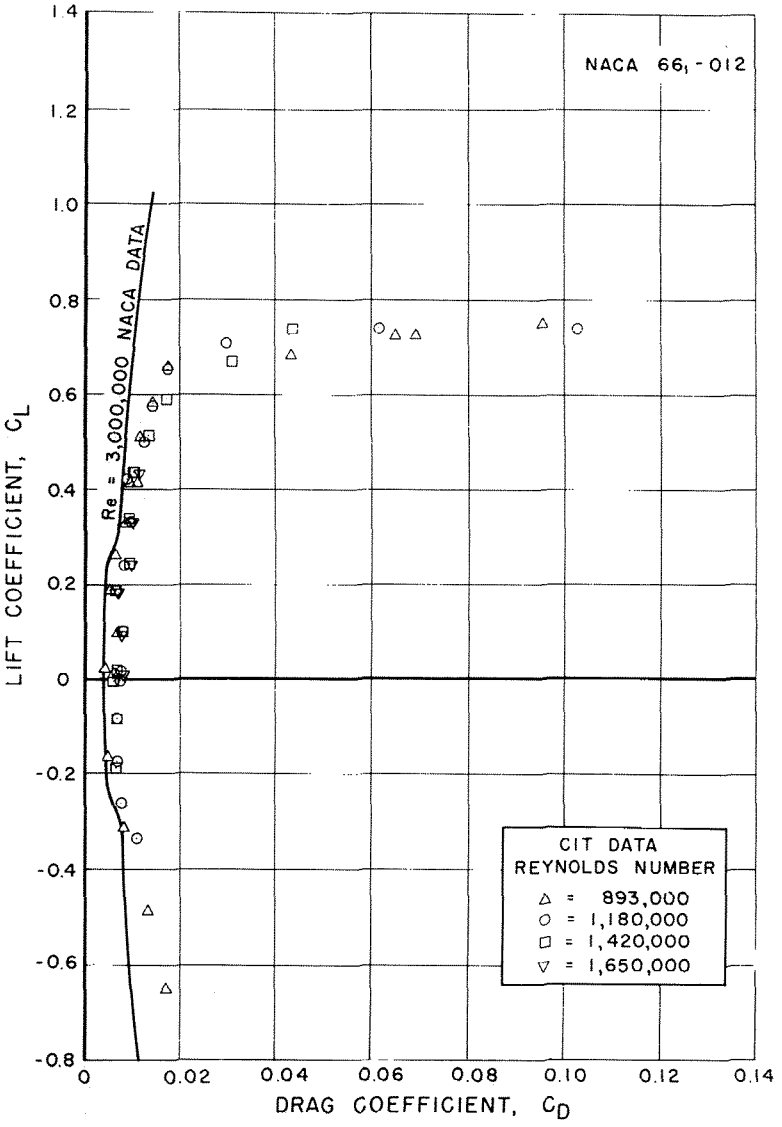


Fig. 3 - Polar diagram for the NACA $66_1$-012 hydrofoil in noncavitating flow.

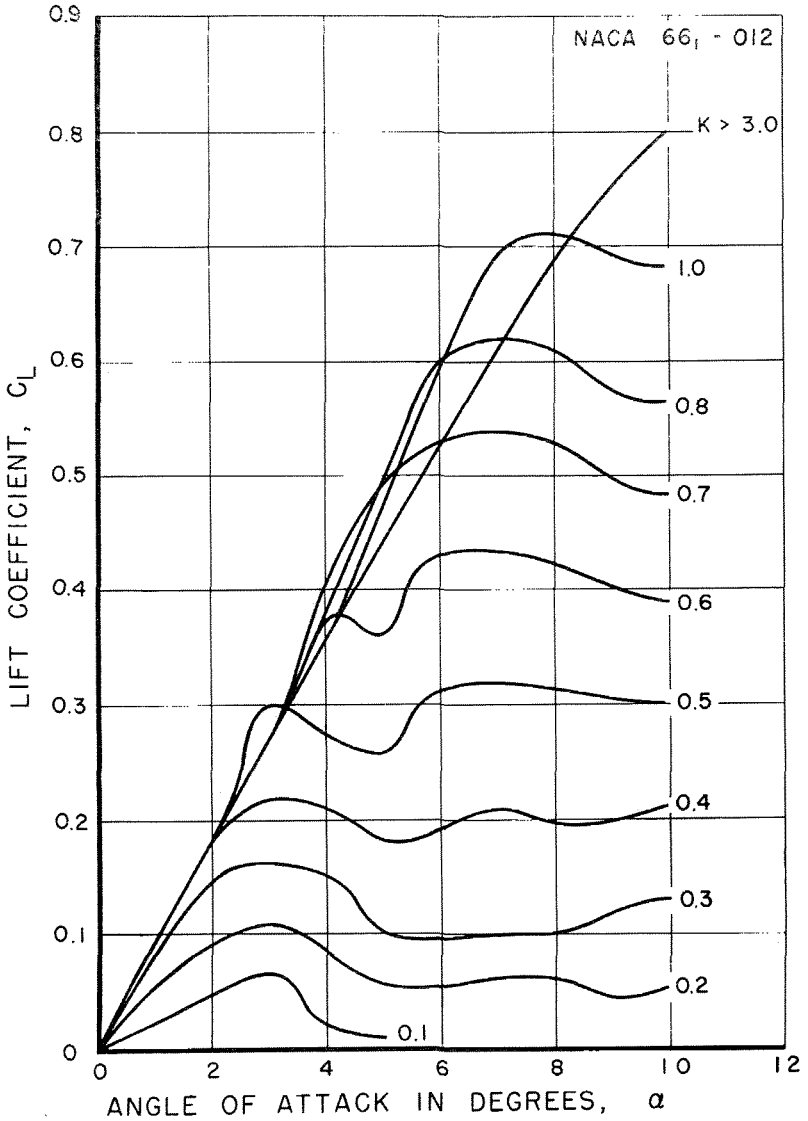


Fig. 4 - Lift coefficient as a function of angle of attack and cavitation number for the NACA $66_1$-012 hydrofoil. These curves are cross plots of the data curves, Fig. 7.

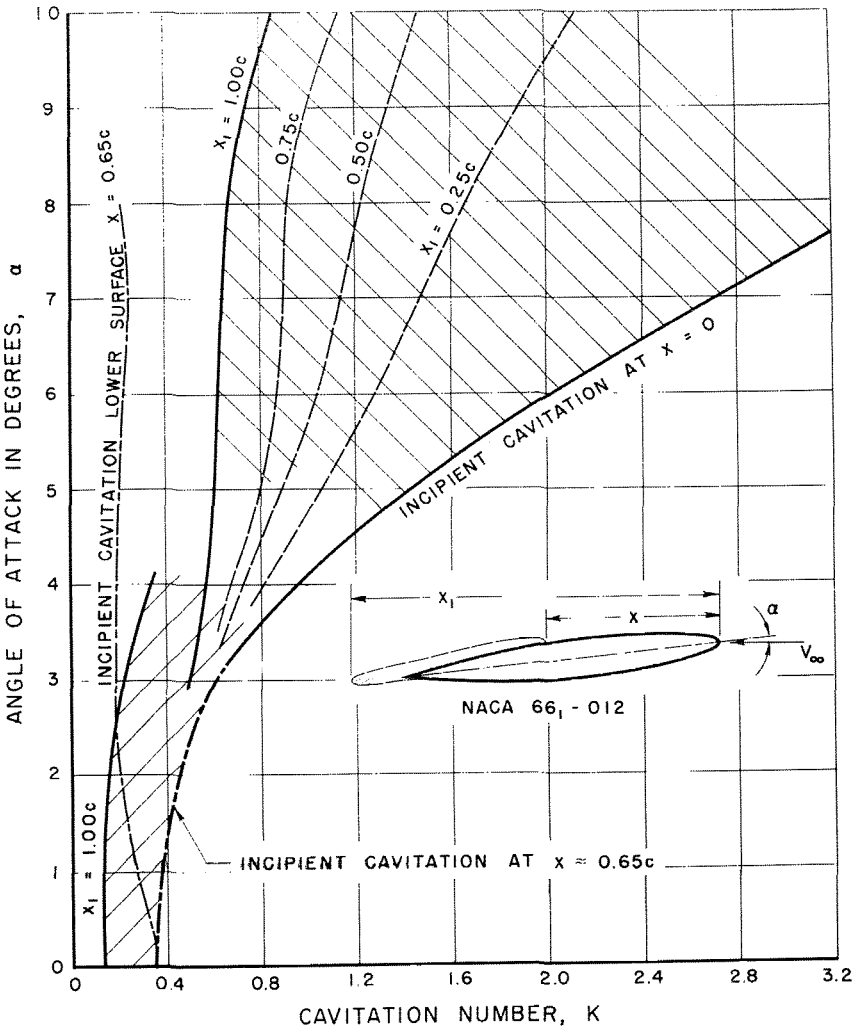


Fig. 5 - Cavitation diagram for the NACA $66_1$-012 hydrofoil.

for noncavitating flow. For angles of attack greater than 3 degrees there is an increase in lift small amounts of cavitation on the hydrofoil. The cavitation diagram, Fig. 5, shows the extent of cavitation on the hydrofoil as a function of angle of attack and cavitation number. At angles of attack up to 3 degrees, the cavitation first appears at approximately the 65 percent chord point, as shown by the lower, broken line. At angles of attack greater than 3 degrees, cavitation began near the leading edge of the hydrofoil. In the region between three and four degrees attack angle, the position of the cavitation on the hydrofoil became unstable and incipient cavitation might occur either at the leading edge or at the 60 percent chord point. After cavitation had been established on the hydrofoil at these attack angles, it would often fluctuate between the leading edge and the 60 percent chord point or the cavitation would separate into long thin individual cavities attached at the leading edge. Figure 6 shows examples of the three patterns of cavitation on the NACA $66_1$-012 hydrofoil at an angle of attack of 3 degrees. In Fig. 6a there is a continuous cavity attached at the leading edge of the hydrofoil. As the cavitation number is reduced, Figs. 6b and 6c, the cavity splits into a number of long individual cavities separated by portions of fully wetted flow. At still lower cavitation numbers the cavitation disappears from the leading edge and begins on the after portion of the hydrofoil, Fig. 6d, e, and f. At the attack angles where the position of the cavitation on the hydrofoil is not stable, the presence of the tunnel walls causes the cavitation to remain attached near the leading edge of the hydrofoil at the walls.

The dashed lines in Fig. 5, noted as $X_1 = 0.25\,c$ to $1.00\,c$ show the extent of the cavitation on the upper surface of the hydrofoil. At $X_1 = 1.00\,c$ the downstream end, or closure, of the cavity just extends to the trailing edge of the model. The region to the left of the $X_1 = 1.00\,c$ line gives the cavitation number for which the hydrofoil is in full cavity flow with the cavity extending downstream from the hydrofoil.

Cavitation occurred on the lower, pressure surface of the hydrofoils for angles of attack up to 8 degrees. The cavitation number at

which the cavitation begins on the lower surface is indicated in Fig. 5. At angles of attack greater than 3 degrees, cavitation did not being on the lower surface until a long, full cavity covered the entire upper surface.

Figure 7 shows lift coefficient as a function of cavitation number at constant angle of attack. Each curve in Fig. 7 represents the results of one test run, and the data points are the measured values of the lift coefficient. Figure 4 is a cross plot of Fig. 7. The dashed line in Fig. 7 shows the cavitation number for incipient cavitation on the upper surface. As noted in Fig. 4, there is an increase in lift coefficient at constant angle of attack when cavitation first begins near the leading edge of the hydrofoil. For small angles of attack where the cavitation begins nearly at the mid-chord point, the lift coefficient decreases as soon as the hydrofoil begins to cavitate.

Figure 8 shows drag coefficient as a function of cavitation number at constant angle of attack. Each curve in Fig. 8 is for the same test run as the data for the corresponding angle of attack in Fig. 7. The drag coefficient increases as soon as cavitation begins on the hydrofoil, reaches a maximum when the cavitation extends approximately to the trailing edge and then decreases as the cavitation number is reduced further.

Lift and drag coefficients at constant cavitation numbers are shown in the cavitation polar diagram, Fig. 9. The dashed lines in Fig. 9 are lines of constant angle of attack. Figure 9, like Fig. 4, was compiled from many test runs in which the velocity and angle of attack were held constant and the cavitation number varied from noncavitating to fully cavitating flow. The drag coefficient has been plotted to a scale ten times that of the lift coefficient in Fig. 9.

Figure 10 shows curves of quarter-chord pitching moment as a function of angle of attack at constant cavitation number. It should be noted that the moment coefficient in Fig. 10 has been plotted to a much expanded scale compared with that for noncavitating flow, Fig. 2, in order to show the changes more clearly. For noncavitating flow with $K > 3.0$ the pitching moment is slightly positive, or nose up. When

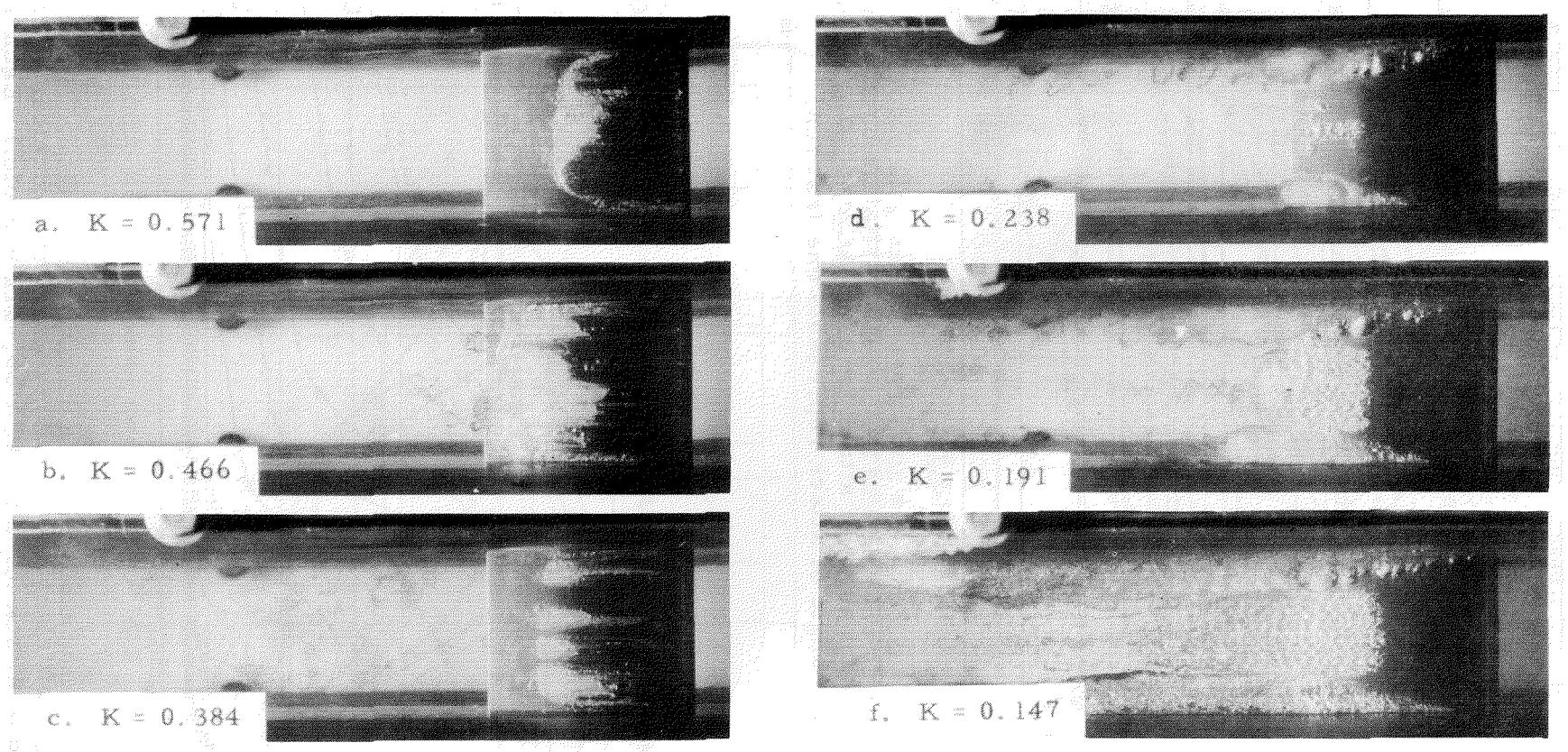


Fig. 6 - Cavitation on the NACA $66_1$-012 hydrofoil at an angle of attack of 3 degrees.

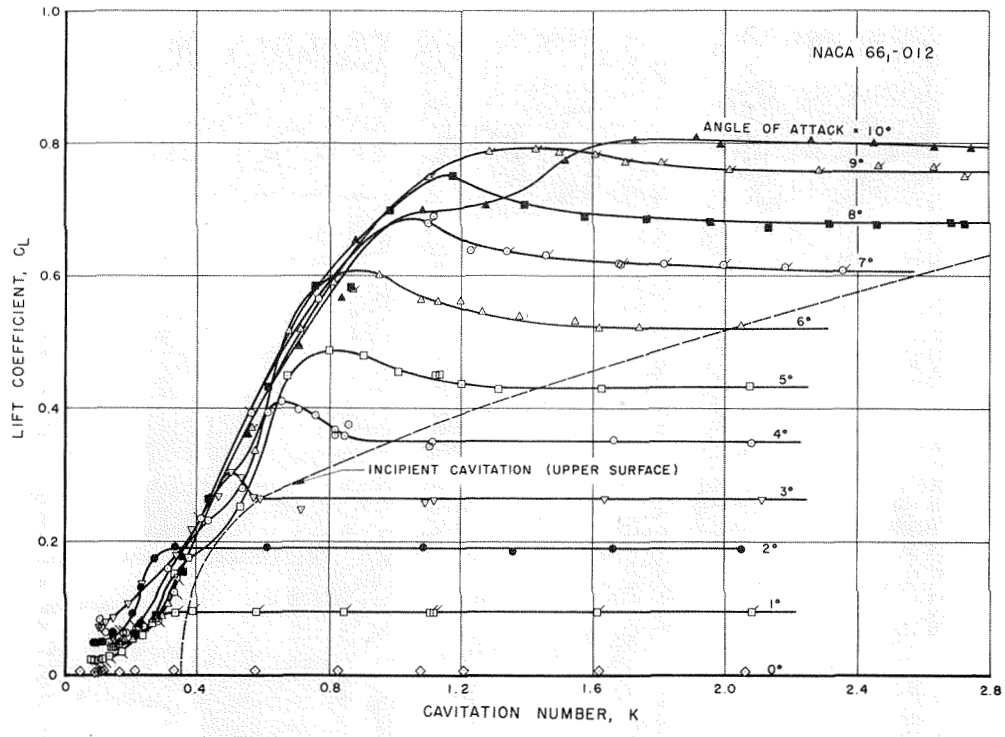


Fig. 7 - Lift coefficient as a function of cavitation number at constant angle of attack for the NACA $66_1$-012 hydrofoil. Each angle of attack represents one test run.

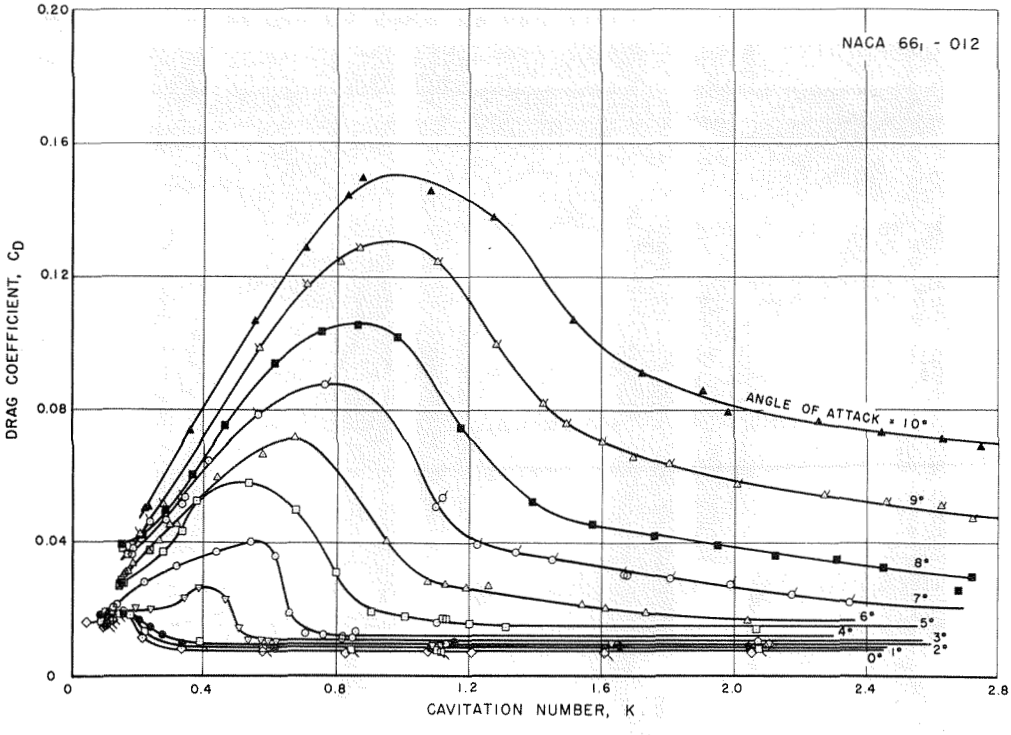


Fig. 8 - Drag coefficient as a function of cavitation number at constant angle of attack for the NACA $66_1$-012 hydrofoil. Each angle of attack represents one test run.

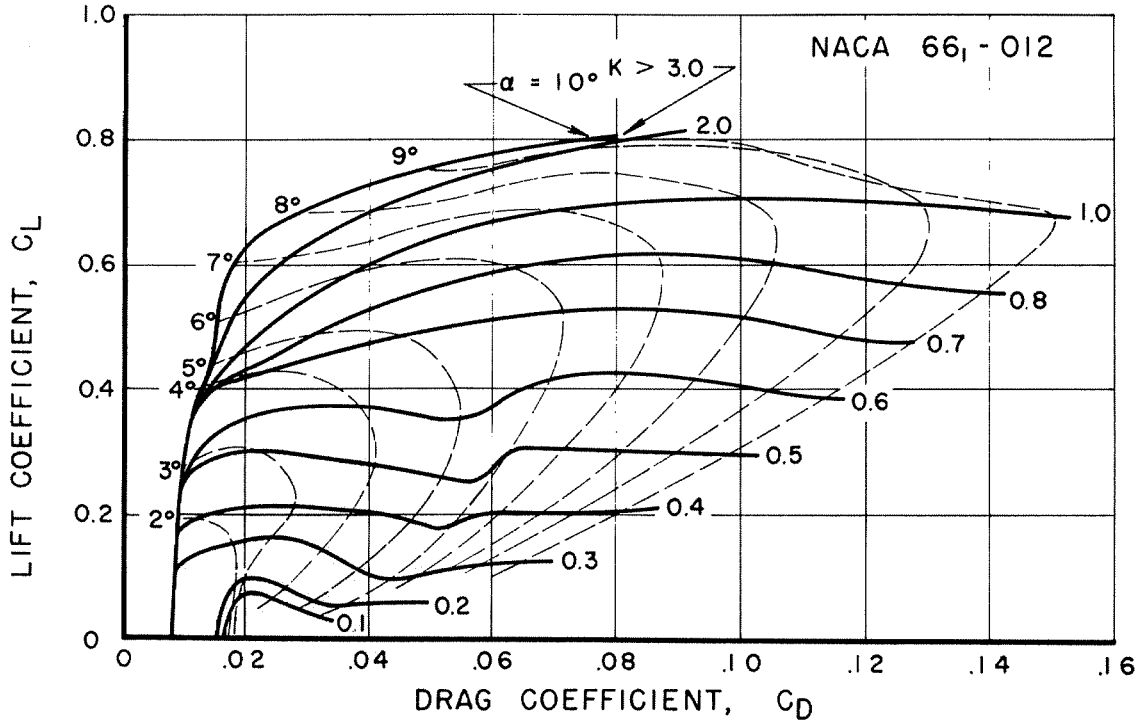


Fig. 9 - Polar diagram for cavitating and noncavitating flow for the NACA $66_1$-012 hydrofoil. These curves are cross plots of the data curves, Fig. 8.

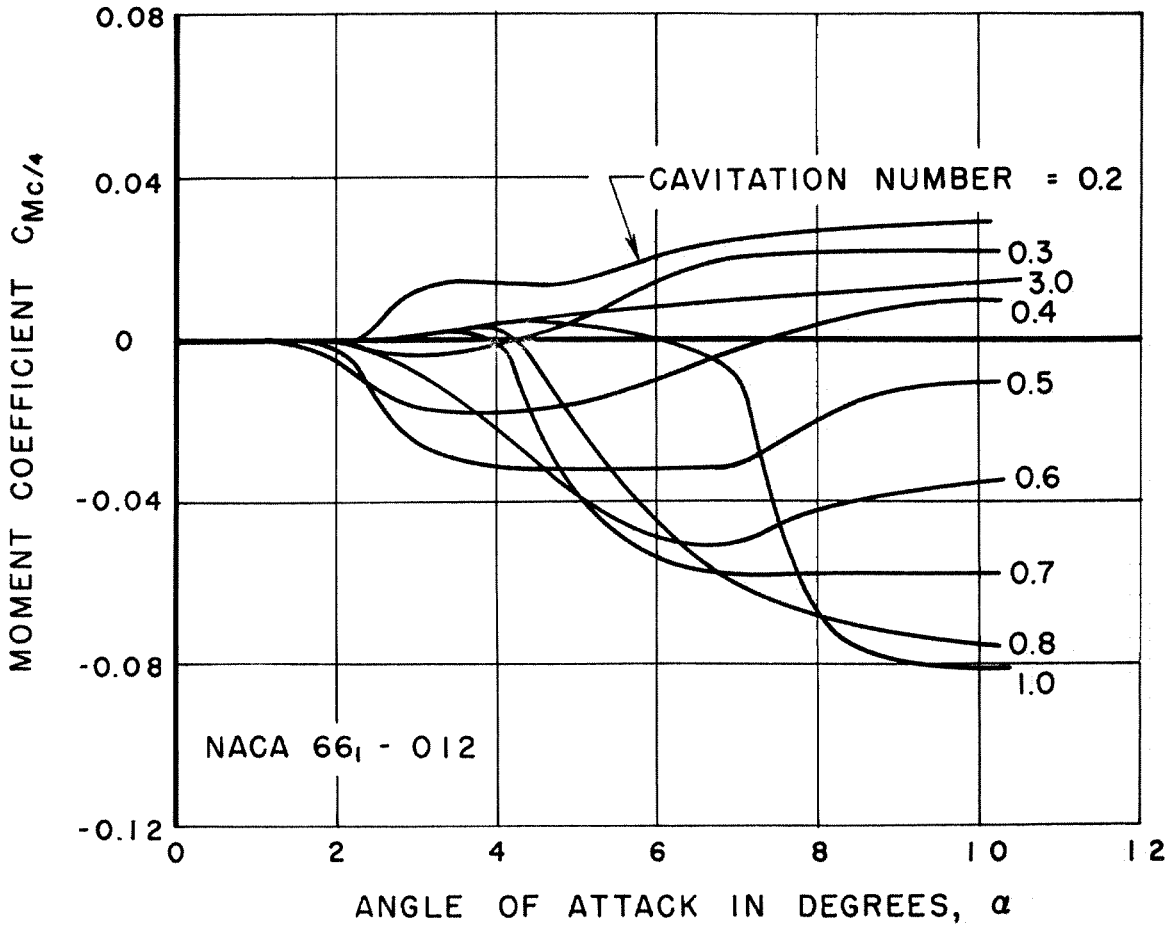


Fig. 10 - Quarter-chord moment coefficient as a function of angle of attack and cavitation number for the NACA $66_1$-012 hydrofoil.

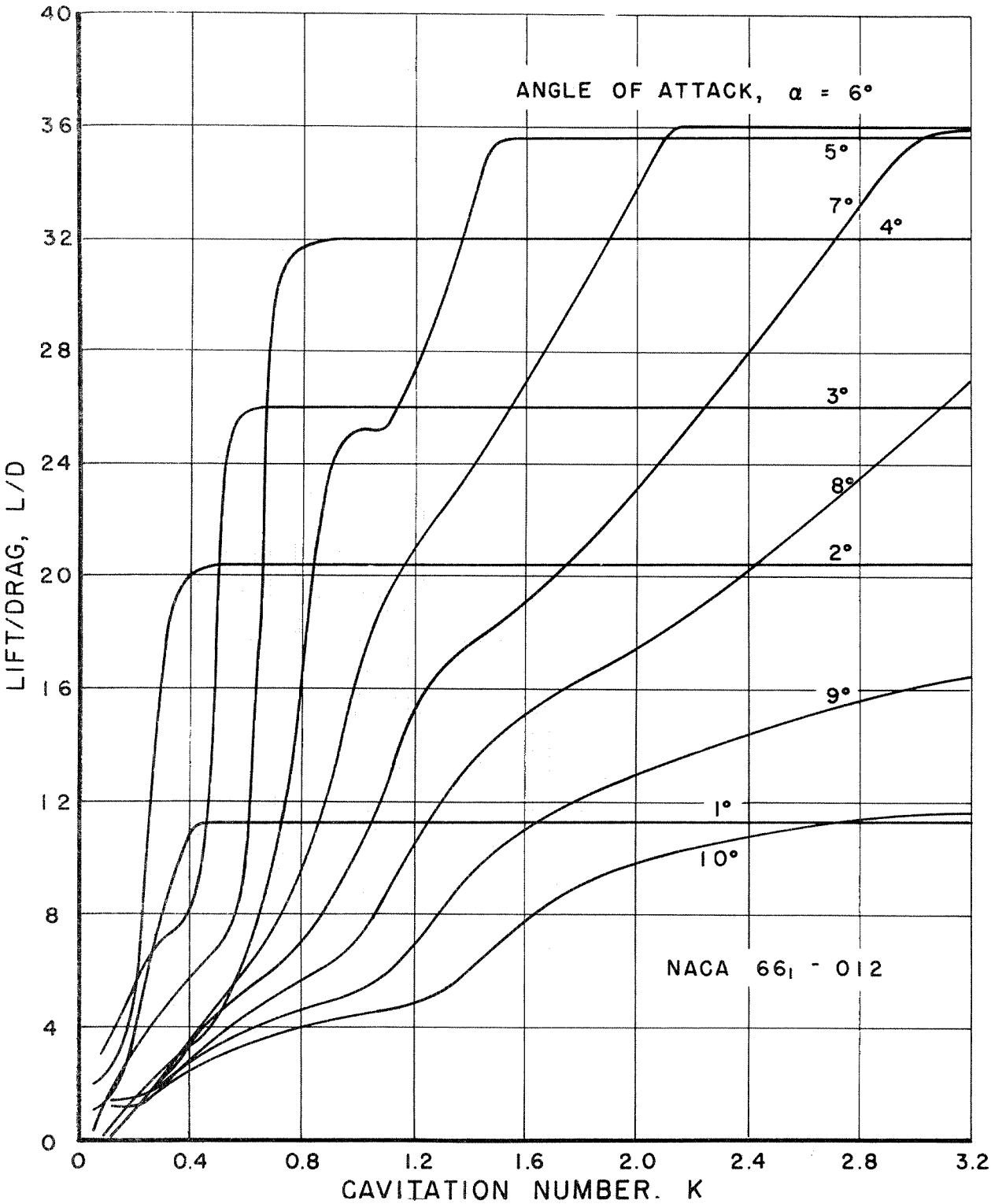


Fig. 11 - Lift/drag ratio as a function of cavitation number and angle of attack for the NACA $66_1$-012 hydrofoil.

cavitation begins at higher attack angles the pitching moment becomes negative, then increases toward the noncavitating value as the cavitation number is decreased, and finally becomes more positive at cavitation numbers less than 0.3. The pitching moment is zero for attack angles less than two degrees for all cavitation numbers.

Figure 11 shows the lift/drag ratio as a function of cavitation number. Each curve in this figure is for a constant angle of attack. The horizontal portions of the curves in Fig. 11 are regions of zero cavitation. When cavitation begins there is a rapid decrease in lift/drag ratio even though Figs. 4 and 7 show an increase in lift with small amounts of cavitation at angles of attack greater than 3 degrees. As cavitation begins, the increase in drag is proportionately greater than the increase in lift. As the cavitation number is reduced to give a large cavity on the hydrofoil, the drag coefficient reaches a maximum and then decreases. The lift coefficient, however, decreases rapidly with cavitation number and the reduction in drag coefficient merely causes a reduction in the slope of the lift/drag ratio curves.

## REFERENCES

1. Kermeen, Robert W., "Water Tunnel Tests of NACA 4412 and Walchner Profile 7 Hydrofoils in Noncavitating and Cavitating Flows", California Institute of Technology, Hydrodynamics Laboratory Report No. 47-5, January 1956.

2. Hotz, G.M. and McGraw, J.T., "The High Speed Water Tunnel Three-Component Force Balance", California Institute of Technology, Hydrodynamics Laboratory Report No. 47-1, January 1955.

3. Abbot, I.H., von Doenhoff, A.E., and Stivers, L.S. Jr., "Summary of Airfoil Data", NACA Report No. 824, 1945.

4. Loftin, L.K. and Smith, H.A., "Aerodynamic Characteristics of 15 NACA Airfoil Sections at Seven Reynolds Numbers from $0.7 \times 10^6$ to $9.0 \times 10^6$", NACA Technical Note 1945, October 1949.

## APPENDIX

## DATA TABLES

I. Section Characteristics of the NACA $66_1$-012 Hydrofoil in Non-cavitating Flow (lift and drag corrected for tunnel interference effects).

V = 31.0 fps  Re = $0.893 \times 10^6$

| $\alpha^o$ | $C_L$ | $C_D$ | $C_M$ |
|---|---|---|---|
| 0 | .004 | .0063 | .000 |
| 1 | .096 | .0062 | -0.001 |
| 2 | .189 | .0051 | -0.002 |
| 3 | .267 | .0062 | .001 |
| 4 | .335 | .0085 | .004 |
| 5 | .419 | .0102 | .005 |
| 6 | .511 | .0116 | .006 |
| 7 | .588 | .0144 | .007 |
| 8 | .666 | .0176 | .009 |
| 9 | .689 | .0434 | .012 |
| 10 | .730 | .0651 | .013 |
| 11 | .751 | .0960 | .002 |
| 12 | .691 | .1460 | -0.027 |
| 13 | .623 | .1733 | -0.054 |
| 10 | .730 | .0694 | .011 |
| 5 | .419 | .0092 | .005 |
| 0 | .015 | .0037 | .000 |
| -2 | -0.169 | .0042 | .000 |
| -4 | -0.315 | .0080 | -0.006 |
| -6 | -0.489 | .0127 | -0.007 |
| -8 | -0.652 | .0166 | -0.007 |
| 0 | .003 | .0050 | -0.001 |

V = 41.2 fps  Re = $1.185 \times 10^6$

| $\alpha^o$ | $C_L$ | $C_D$ | $C_M$ |
|---|---|---|---|
| 0 | -0.002 | .0071 | .000 |
| 1 | .091 | .0070 | -0.001 |
| 2 | .184 | .0064 | -0.001 |
| 3 | .247 | .0087 | .004 |
| 4 | .331 | .0099 | .005 |
| 5 | .416 | .0109 | .005 |
| 6 | .503 | .0125 | .006 |
| 7 | .582 | .0143 | .007 |
| 8 | .653 | .0177 | .010 |
| 9 | .713 | .0297 | .012 |
| 10 | .742 | .0616 | .017 |
| 11 | .746 | .1032 | .004 |
| 5 | .423 | .0087 | .005 |
| 0 | .011 | .0069 | -0.001 |
| -1 | -0.082 | .0064 | -0.001 |
| -2 | -0.175 | .0066 | .000 |
| -3 | -0.261 | .0073 | -0.002 |
| -4 | -0.334 | .0106 | -0.006 |
| 0 | -0.004 | .0068 | -0.001 |

V = 49.5 fps  Re = $1.425 \times 10^6$

| $\alpha^o$ | $C_L$ | $C_D$ | $C_M$ |
|---|---|---|---|
| 0 | -0.005 | .0058 | .000 |
| 1 | .092 | .0073 | -0.001 |
| 2 | .188 | .0066 | -0.002 |
| 3 | .248 | .0090 | .003 |
| 4 | .341 | .0097 | .004 |
| 5 | .433 | .0108 | .004 |
| 6 | .519 | .0121 | .004 |
| 7 | .595 | .0171 | .006 |
| 8 | .671 | .0309 | .009 |
| 9 | .742 | .0438 | .014 |
| 5 | .439 | .0106 | .003 |
| 0 | .011 | 0066 | -0.001 |
| -1 | -0.088 | .0062 | .000 |
| -2 | -0.186 | .0062 | .001 |
| 0 | .004 | .0068 | .001 |

V = 57.4 fps  Re = $1.650 \times 10^6$

| $\alpha^o$ | $C_L$ | $C_D$ | $C_M$ |
|---|---|---|---|
| 0 | -0.007 | .0076 | .000 |
| 1 | .090 | .0078 | -0.001 |
| 2 | .185 | .0071 | -0.002 |
| 3 | .247 | .0093 | .004 |
| 4 | .338 | .0100 | .004 |
| 5 | .434 | .0113 | .004 |

II. Force Characteristics of the NACA $66_1$-012 Hydrofoil in Cavitating Flow (data not corrected for tunnel interference effects; cavitation number based on vapor pressure).

V = 40 fps  $\alpha = -1^o$

| K | $C_L$ | $C_D$ | $C_M$ |
|---|---|---|---|
| 2.966 | -0.106 | .0078 | .001 |
| 2.056 | -0.108 | .0078 | .001 |
| 1.613 | -0.110 | .0076 | .001 |
| 1.251 | -0.109 | .0075 | .001 |
| 1.030 | -0.112 | .0071 | .001 |
| 0.935 | -0.111 | .0071 | .002 |
| .859 | -0.110 | .0066 | .002 |
| .757 | -0.111 | .0074 | .002 |
| .635 | -0.111 | .0074 | .002 |
| .530 | -0.111 | .0076 | .002 |
| .419 | -0.111 | .0081 | .002 |
| .315 | -0.114 | .0084 | .003 |
| .264 | -0.110 | .0100 | .005 |
| .209 | -0.076 | .0148 | .004 |
| .183 | -0.056 | .0175 | -0.002 |
| .156 | -0.043 | .0187 | -0.005 |
| .129 | -0.033 | .0168 | -0.005 |
| .108 | -0.030 | .0161 | -0.004 |
| .103 | -0.028 | .0164 | -0.004 |
| .103 | -0.028 | .0162 | -0.004 |
| .099 | -0.028 | .0161 | -0.004 |
| .101 | -0.028 | .0158 | -0.004 |
| .099 | -0.029 | .0157 | -0.004 |
| .100 | -0.029 | .0132 | -0.004 |
| .111 | -0.027 | .0165 | -0.004 |
| .368 | -0.112 | .0080 | .003 |
| .607 | -0.111 | .0072 | .003 |
| 1.098 | -0.114 | .0074 | |
| 1.098 | -0.114 | .0076 | .002 |
| 1.627 | -0.110 | .0079 | .002 |
| 2.928 | -0.108 | .0074 | .001 |

V = 40 fps  $\alpha = 0^o$

| K | $C_L$ | $C_D$ | $C_M$ |
|---|---|---|---|
| 2.061 | -0.005 | .0073 | -0.001 |
| 1.617 | -0.005 | .0073 | -0.001 |
| 1.080 | -0.005 | .0078 | -0.001 |
| 0.829 | -0.005 | .0070 | -0.001 |
| .577 | -0.006 | .0073 | .000 |
| .331 | -0.006 | .0081 | .000 |
| .212 | -0.005 | .0116 | .000 |
| .168 | -0.003 | .0189 | -0.001 |
| .120 | -0.004 | .0173 | .000 |
| .101 | -0.004 | .0161 | .000 |
| .099 | -0.004 | .0158 | .000 |
| .095 | -0.003 | .0162 | .000 |
| .091 | -0.003 | .0159 | .000 |
| .044 | -0.004 | .0163 | .000 |
| .112 | -0.003 | .0166 | .000 |
| 1.210 | -0.006 | .0071 | -0.001 |
| 2.934 | -0.004 | .0083 | -0.001 |

V = 40 fps  $\alpha = 1^o$

| K | $C_L$ | $C_D$ | $C_M$ |
|---|---|---|---|
| 2.984 | .094 | .0099 | -0.001 |
| 2.081 | .093 | .0086 | -0.001 |
| 1.615 | .092 | .0075 | -0.001 |
| 1.106 | .092 | .0080 | -0.001 |
| 0.844 | .091 | .0080 | -0.001 |
| .580 | .091 | .0087 | -0.001 |
| .336 | .092 | .0095 | -0.001 |
| .220 | .065 | .0136 | -0.001 |
| .174 | .032 | .0183 | .006 |
| .139 | .025 | .0183 | .006 |
| .115 | .023 | .0166 | .006 |
| .102 | .023 | .0159 | .004 |
| .089 | .020 | .0173 | .005 |
| .092 | .020 | .0157 | .006 |
| .089 | .021 | .0164 | .006 |
| .387 | .093 | .0106 | .000 |
| 1.119 | .092 | .0077 | .000 |
| 2.984 | .095 | .0091 | -0.001 |

II. (cont.) Force Characteristics of the NACA $66_1$-012 Hydrofoil in Cavitating Flow (data not corrected for tunnel interference effects; cavitation number based on vapor pressure).

V = 40 fps, $\alpha = 2^\circ$

| K | $C_L$ | $C_D$ | $C_M$ |
|---|---|---|---|
| 2.984 | .193 | .0098 | -0.002 |
| 2.051 | .189 | .0092 | -0.002 |
| 1.662 | .189 | .0092 | -0.002 |
| 1.089 | .189 | .0089 | -0.002 |
| 0.612 | .190 | .0089 | -0.002 |
| .336 | .190 | .0099 | -0.003 |
| .272 | .173 | .0124 | -0.005 |
| .235 | .129 | .0144 | -0.004 |
| .202 | .090 | .0169 | .019 |
| .147 | .060 | .0193 | .019 |
| .110 | .048 | .0179 | .030 |
| .104 | .047 | .0174 | .030 |
| .098 | .048 | .0171 | .032 |
| .102 | .047 | .0181 | .031 |
| .100 | .046 | .0179 | .026 |
| .095 | .047 | .0179 | .036 |
| .083 | .044 | .0186 | .036 |
| .112 | .046 | .0197 | .031 |
| 1.160 | .183 | .0103 | .020 |
| 2.984 | .189 | .0103 | .007 |

V = 41 fps, $\alpha = 3^\circ$

| K | $C_L$ | $C_D$ | $C_M$ |
|---|---|---|---|
| 2.973 | .267 | .0102 | .003 |
| 2.112 | .263 | .0103 | .003 |
| 1.639 | .262 | .0101 | .002 |
| 1.119 | .260 | .0097 | .004 |
| 0.592 | .263 | .0108 | .004 |
| .571 | .266 | .0109 | .003 |
| .535 | .295 | .0111 | -0.001 |
| .504 | .304 | .0149 | -0.007 |
| .466 | .266 | .0233 | -0.023 |
| .384 | .216 | .0267 | -0.015 |
| .340 | .176 | .0232 | -0.009 |
| .238 | .135 | .0200 | .004 |
| .191 | .103 | .0202 | .016 |
| .147 | .084 | .0194 | .016 |
| .123 | .077 | .0185 | .015 |
| .110 | .067 | .0186 | .015 |
| .104 | .072 | .0185 | .016 |
| .617 | .246 | .0104 | .007 |
| 1.092 | .257 | .0097 | .005 |
| 2.925 | .258 | .0101 | .005 |

V = 40 fps, $\alpha = 4^\circ$

| K | $C_L$ | $C_D$ | $C_M$ |
|---|---|---|---|
| 3.049 | .353 | .0111 | .005 |
| 2.080 | .347 | .0105 | .005 |
| 1.662 | .352 | | .004 |
| 1.131 | .349 | .0099 | .004 |
| 0.848 | .358 | .0113 | .005 |
| .816 | .358 | .0111 | .005 |
| .819 | .367 | .0117 | .005 |
| .859 | .374 | .0121 | .004 |
| .758 | .389 | .0124 | .003 |
| .703 | .397 | .0129 | .001 |
| .656 | .410 | .0190 | -0.009 |
| .539 | .279 | .0402 | -0.035 |
| .435 | .231 | .0371 | -0.019 |
| .314 | .157 | .0329 | -0.003 |
| .219 | .067 | .0282 | .013 |
| .133 | .047 | .0216 | .015 |
| .132 | .046 | .0215 | .014 |
| .122 | .061 | .0204 | .015 |
| .107 | .080 | .0171 | .017 |
| .611 | .393 | .0360 | -0.021 |
| 1.105 | .341 | .0162 | .004 |
| 2.996 | .344 | .0101 | .004 |

V = 40 fps, $\alpha = 5^\circ$

| K | $C_L$ | $C_D$ | $C_M$ |
|---|---|---|---|
| 2.955 | .437 | .0148 | .005 |
| 2.077 | .434 | .0145 | .004 |
| 1.625 | .429 | | .004 |
| 1.313 | .428 | .0149 | .005 |
| 1.202 | .436 | .0160 | .005 |
| 1.122 | .448 | .0176 | .005 |
| 1.008 | .451 | .0180 | .005 |
| 0.903 | .478 | .0193 | .004 |
| .799 | .486 | .0310 | -0.004 |
| .674 | .448 | .0498 | -0.041 |
| .534 | .252 | .0580 | -0.033 |
| .375 | .175 | .0525 | -0.009 |
| .277 | .089 | .0375 | .009 |
| .231 | .057 | .0386 | .010 |
| .168 | .044 | .0365 | .011 |
| .147 | .040 | .0285 | .015 |
| .151 | .040 | .0381 | .016 |
| .148 | .039 | .0277 | .016 |
| .142 | .039 | .0284 | .016 |
| .331 | .150 | .0431 | -0.003 |
| 1.132 | .451 | .0173 | .005 |
| 2.980 | .437 | .0137 | .004 |

V = 40 fps, $\alpha = 6^\circ$

| K | $C_L$ | $C_D$ | $C_M$ |
|---|---|---|---|
| 2.955 | .534 | .0149 | .006 |
| 2.048 | .522 | .0166 | .007 |
| 1.739 | .520 | .0192 | .006 |
| 1.617 | .520 | .0202 | .006 |
| 1.545 | .529 | .0213 | .006 |
| 1.378 | .537 | | .007 |
| 1.261 | .543 | .0270 | .007 |
| 1.196 | .560 | .0261 | .007 |
| 1.077 | .562 | .0281 | .005 |
| 0.950 | .600 | .0404 | -0.007 |
| .675 | .513 | .0714 | -0.056 |
| .575 | .335 | .0662 | -0.042 |
| .438 | .269 | .0597 | -0.018 |
| .316 | .104 | .0455 | .013 |
| .261 | .076 | .0404 | .016 |
| .232 | .066 | .0379 | .018 |
| .183 | .052 | .0336 | .016 |
| .170 | .050 | .0318 | .016 |
| .164 | .050 | .0314 | .016 |
| .162 | .049 | .0311 | .016 |
| .152 | .049 | .0305 | .017 |
| .296 | .084 | .0427 | .016 |
| 1.129 | .558 | .0275 | .005 |
| 2.968 | .522 | .0144 | .005 |

V = 40 fps, $\alpha = 7^\circ$

| K | $C_L$ | $C_D$ | $C_M$ |
|---|---|---|---|
| 2.930 | .609 | .0171 | .007 |
| 2.353 | .606 | .0223 | .006 |
| 2.180 | .611 | .0248 | .007 |
| 1.993 | .615 | .0276 | .008 |
| 1.811 | .616 | .0294 | .009 |
| 1.684 | .615 | .0304 | .009 |
| 1.453 | .628 | .0348 | .009 |
| 1.336 | .635 | .0370 | .008 |
| 1.227 | .637 | .0393 | .006 |
| 1.100 | .678 | .0509 | -0.009 |
| 0.762 | .564 | .0874 | -0.067 |
| .563 | .391 | .0781 | -0.042 |
| .410 | .232 | .0646 | -0.012 |
| .332 | .120 | .0517 | .015 |
| .282 | .076 | .0469 | .022 |
| .235 | .069 | .0432 | .020 |
| .185 | .060 | .0385 | .017 |
| .184 | .057 | .0386 | .017 |
| .180 | .058 | .0368 | .017 |
| .180 | .056 | .0363 | .017 |
| .340 | .144 | .0537 | .011 |
| 1.119 | .687 | .0539 | -0.009 |
| 1.675 | .617 | .0304 | .009 |
| 2.955 | .602 | .0171 | .007 |

V = 31 fps, $\alpha = 8^\circ$

| K | $C_L$ | $C_D$ | $C_M$ |
|---|---|---|---|
| 5.198 | .674 | .0218 | .010 |
| 3.565 | .682 | .0227 | .008 |
| 2.683 | .682 | .0262 | .010 |
| 2.459 | .676 | .0330 | .011 |
| 2.314 | .679 | .0353 | .011 |
| 2.130 | .672 | .0363 | .011 |
| 1.954 | .681 | .0397 | .012 |
| 1.761 | .685 | .0425 | .012 |
| 1.577 | .688 | .0457 | .012 |
| 1.393 | .707 | .0522 | .008 |
| 1.178 | .750 | .0741 | -0.024 |
| 0.986 | .696 | .1017 | -0.071 |
| .753 | .583 | .1035 | -0.065 |
| .612 | .432 | .0938 | -0.047 |
| .463 | .264 | .0751 | -0.012 |
| .361 | .152 | .0603 | .010 |
| .280 | .086 | .0500 | .024 |
| .211 | .060 | .0424 | .022 |
| .148 | .060 | .0396 | .020 |
| .861 | .581 | .1055 | -0.073 |
| 2.724 | .678 | .0303 | .011 |
| 5.269 | .690 | .0244 | .011 |

V = 31 fps, $\alpha = 9^\circ$

| K | $C_L$ | $C_D$ | $C_M$ |
|---|---|---|---|
| 5.323 | .756 | .0522 | .010 |
| 3.680 | .750 | .0518 | .009 |
| 3.614 | .768 | .0431 | .006 |
| 3.195 | .355 | .0448 | .009 |
| 2.946 | .754 | .0465 | .009 |
| 2.837 | .749 | .0473 | .009 |
| 2.631 | .763 | .0516 | .010 |
| 2.465 | .764 | .0527 | .010 |
| 2.277 | .759 | .0543 | .010 |
| 2.013 | .758 | .0574 | .010 |
| 1.808 | .770 | .0634 | .008 |
| 1.699 | .770 | .0654 | .006 |
| 1.605 | .783 | .0700 | .002 |
| 1.499 | .785 | .0754 | -0.003 |
| 1.427 | .790 | .0816 | -0.010 |
| 1.285 | .785 | .0991 | -0.025 |
| 1.105 | .747 | .1242 | -0.073 |
| 0.870 | .578 | .1286 | -0.080 |
| .710 | .517 | .1175 | -0.060 |
| .567 | .370 | .0992 | -0.030 |
| .273 | .084 | .0512 | .025 |
| .202 | .050 | .0423 | .027 |
| .810 | .587 | .1241 | -0.076 |
| 2.727 | .748 | .0478 | .010 |
| 5.287 | .740 | .0509 | .011 |

V = 31 fps, $\alpha = 10^\circ$

| K | $C_L$ | $C_D$ | $C_M$ |
|---|---|---|---|
| 5.377 | .802 | .0841 | .013 |
| 3.670 | .791 | .0757 | .013 |
| 3.226 | .794 | .0782 | .012 |
| 3.212 | .802 | .0692 | .015 |
| 2.950 | .786 | .0685 | .014 |
| 2.848 | .793 | .0709 | .014 |
| 2.633 | .793 | .0713 | .014 |
| 2.451 | .800 | .0733 | .013 |
| 2.260 | .803 | .0766 | .012 |
| 1.989 | .797 | .0793 | .010 |
| 1.912 | .807 | .0854 | .007 |
| 1.726 | .804 | .0908 | .001 |
| 1.518 | .773 | .1067 | -0.015 |
| 1.277 | .704 | .1377 | -0.046 |
| 1.084 | .697 | .1454 | -0.076 |
| 0.877 | .651 | .1496 | -0.083 |
| .703 | .491 | .1283 | -0.056 |
| .553 | .360 | .1067 | -0.021 |
| .359 | .175 | .0736 | .014 |
| .230 | .077 | .0509 | .027 |
| .220 | .073 | .0503 | .029 |
| .832 | .564 | .1441 | -0.080 |
| 2.748 | .787 | .0692 | .013 |
| 5.330 | .769 | .0739 | .008 |

DISTRIBUTION LIST FOR TECHNICAL REPORTS ISSUED UNDER CONTRACT NONR-220(12)

| Item | Address | No. Copies |
|---|---|---|
| 1 | Commanding Officer and Director, David Taylor Model Basin, Washington 7, D.C., Attn: Code 580 | 54 |
| 2 | Chief of Naval Research, Office of Naval Research, Department of the Navy, Washington 25, D.C., Attn: Mechanics Branch (Code 438) | 6 |
| 3 | Commanding Officer, Branch Office, Office of Naval Research, 495 Summer St., Boston 10, Mass. | 1 |
| 4 | Commanding Officer, Branch Office, Office of Naval Research, 346 Broadway, New York 13, N. Y. | 1 |
| 5 | Commanding Officer, Branch Office, Office of Naval Research, The John Crerar Library Bldg., 10th Floor, 86 E. Randolph St., Chicago 1, Ill. | 1 |
| 6 | Commanding Officer, Bran ch Office, Office of Naval Research, 1000 Geary St., San Francisco 9, Calif. | 1 |
| 7 | Commanding Officer, Branch Office, Office of Naval Research, 1030 E. Green Street, Pasadena 1, Calif. | 2 |
| 8 | Asst. Naval Attache for Research, Office of Naval Research, American Embassy, London, England, Navy 100, F.P.O. New York, N.Y. | 2 |
| 9 | Director, Naval Research Laboratory, Office of Naval Research, Washington 25, D.C. Attn: Librarian | 9 |
| 10 | Bureau of Aeronautics, Dept. of the Navy, Washington 25, D.C., Attn: Aero and Hydro Branch (Code AD3) | 2 |
| 11 | Bureau of Ordnance, Dept. of the Navy, Washington 25, D.C., Attn: Code Re9<br>Code Re6<br>Code Re3 | 1<br>1<br>1 |
| 12 | Commander, U.S. Naval Ordnance Laboratory, U.S. Navy Bureau of Ordnance, White Oak, Silver Spring 19, Maryland | 2 |
| 13 | Underwater Ordnance Dept., Naval Ordnance Test Station, 3202 E. Foothill Blvd., Pasadena, Calif. Attn: Pasadena Annex Library (Code P 5507) | 3 |
| 14 | Chief, Bureau of Ships, Dept. of the Navy, Washington 25, D.C. Attn: Technical Library (Code 312) for additional distribution to: | 10 |

Distribution List (continued)

| Item | Address | No. Copies |
|---|---|---|
| | (Bureau of Ships distribution)<br>Research and Development (Code 300)<br>Ship Design (Code 410)<br>Preliminary Design (Code 420)<br>Hull Design (Code 440)<br>Hull Scientific (Code 442)<br>Propeller Design (Code 554) | |
| 15 | Mr. R. H. Kent, Ballistic Research Laboratories, Dept. of the Army, Aberdeen Proving Ground, Maryland | 1 |
| 16 | Director of Research, National Advisory Committee for Aeronautics, 1512 H Street, N.W., Washington 25, D.C. | 1 |
| 17 | Director, Langley Aeronautical Lab., National Advisory Committee for Aeronautics, Langley Field, Virginia | 1 |
| 18 | Commander, Naval Ordnance Test Station, Inyokern, China Lake, Calif., Attn: Library (Code 5507) | 1 |
| 19 | Dr. K.S.M. Davidson, Experimental Towing Tank, Stevens Institute of Technology, Hoboken, N. J. | 1 |
| 20 | Dr. J.H. McMillen, National Science Foundation, 1520 H Street, N.W., Washington 25, D.C. | 1 |
| 21 | Dr. A. Miller, Bureau of Ordnance (Code Re3d) Navy Dept. Washington 25, D.C. | 1 |
| 22 | Dr. H. Rouse, Iowa Institute of Hydraulic Research, State University of Iowa, Iowa City, Iowa | 1 |
| 23 | Dr. R.G. Folsom, Director, Engineering Research Institute, University of Michigan, East Engineering Bldg. Ann Arbor, Michigan | 1 |
| 24 | Dr. V.L. Streeter, Engineering Dept., University of Michigan, Ann Arbor, Michigan | 1 |
| 25 | Dr. G.F. Wislicenus, Pennsylvania State University, Ordnance Research Laboratory, University Park, Pa. | 1 |
| 26 | Dr. A.T. Ippen, Dept. of Civil and Sanitary Engineering, Massachusetts Institute of Technology, Cambridge 39, Mass. | 1 |
| 27 | Dr. L.G. Straub, St. Anthony Falls Hydraulic Laboratory, University of Minnesota, Minneapolis 14, Minn. | 1 |
| 28 | Prof. K.E. Schoenherr, University of Notre Dame, College of Engineering, Notre Dame, Indiana | 1 |
| 29 | Director, Ordnance Research Laboratory, Pennsylvania State University, University Park, Pa. | 1 |

Distribution List (continued)

| Item | Address | No. Copies |
|---|---|---|
| 30 | Society of Naval Architects and Marine Engineers 74 Trinity Place, New York 6, N.Y. | 1 |
| 31 | Prof. J.K. Vennard, Stanford University, Dept. of Civil Engineering, Stanford, California | 1 |
| 32 | Prof. J.L. Hooper, Worcester Polytechnic Institute, Alden Hydraulic Laboratory, Worcester 6, Mass. | 1 |
| 33 | Prof. J.M. Robertson, Dept. of Theoretical and Applied Mechanics, University of Illinois, Urbana, Ill. | 1 |
| 34 | Dr. A.B. Kinzel, President, Union Carbide and Carbon Research Lab., Inc., 30 E. 42nd St., New York, N.Y. | 1 |
| 35 | Goodyear Aircraft Corp., Akron 15, Ohio, Attn: Security Officer | 1 |
| 36 | Prof. H.R. Henry, Hydraulics Laboratory, Michigan State College, East Lansing, Michigan | 1 |
| 37 | British Joint Services Mission, Navy Staff, Via: David Taylor Model Basin, Code 580, Navy Department, Washington 7, D.C. | 9 |
| 38 | Commander, Submarine Development Group TWO, Box 70, U.S. Naval Submarine Base, New London, Conn. | 1 |
| 39 | Commanding Officer and Director, U.S. Navy Engineering Experiment Station, Annapolis, Maryland | 1 |
| 40 | Library of Congress, Washington 25, D.C., Attn: ASTIA | 1 |
| 41 | Dr. P. R. Garabedian, Stanford University, Applied Mathematics and Statistics Laboratory, Stanford, California | 1 |
| 42 | Armed Services Technical Information Agency, Knott Building, Dayton, Ohio | 5 |
| 43 | Mr. J.G. Baker, Baker Manufacturing Company, Evansville, Wisconsin | 1 |
| 44 | Mr. T.M. Buerman, Gibbs and Cox, Inc., 21 West St., New York 6, New York | 1 |
| 45 | Dynamic Developments, Inc., St. Mark's Lane, Islip, Long Island, New York, Attn: Mr. W.P. Carl, Jr. | 1 |
| 46 | Hydrodynamics Research Laboratory, Consolidated-Vultee Aircraft Corporation, San Diego 12, California | 1 |

Distribution List (continued)

| Item | Address | No. Copies |
|---|---|---|
| 47 | Mr. R.K. Johnston, Miami Shipbuilding Corporation, 615 S.W. Second Avenue, Miami 36, Florida | 1 |
| 48 | Mr. J.D. Pierson, The Glenn L. Martin Company, Baltimore 3, Maryland | 1 |
| 49 | Mr. W.R. Ryan, Edo Corporation, College Point 56, Long Island, New York | 1 |
| 50 | Dr. Robert C. Seamans, Radio Corporation of America, Waltham, Massachusetts | 1 |
| 51 | Dr. A.G. Strandhagen, Department of Engineering Mechanics, University of Notre Dame, Notre Dame, Ind. | 1 |
| 52 | Dr. H.W.E. Lerbs, Hamburgische Schiffbau-Versuchsanstalt Hamburg 33, Bramfelderstrasse 164 | 1 |
| 53 | Commander, Air Research and Development Command, P.O. Box 1395, Baltimore, Maryland. Attn: RDTDED | 1 |
| 54 | Avco Manufacturing Corp., Advanced Development Div., 2385 Revere Beach Parkway, Everett 49, Mass. Atten: Technical Librarian | 1 |
| 55 | Dr. L. Landweber, Iowa Inst. of Hydraulic Research, State University of Iowa, Iowa City, Ia. | 1 |